Journal of Colloid and Interface Science 574 (2020) 430–440

Contents lists available at ScienceDirect

Journal of Colloid and Interface Science

journal homepage: www.elsevier.com/locate/jcis

Nanostructure generation during milk digestion in presence of a cell culture model simulating the small intestine

Claudia Hempt [a,b,1], Mark Gontsarik [c,1], Tina Buerki-Thurnherr [a], Cordula Hirsch [a], Stefan Salentinig [d,*]

[a] Laboratory for Particles-Biology Interactions, Empa, Swiss Federal Laboratories for Materials Science and Technology, Lerchenfeldstrasse 5, 9014 St. Gallen, Switzerland
[b] Department of Health Sciences and Technology, ETH Zürich, Zürich, Switzerland
[c] Laboratory for Biointerfaces, Empa, Swiss Federal Laboratories for Materials Science and Technology, Lerchenfeldstrasse 5, 9014 St. Gallen, Switzerland
[d] Department of Chemistry, University of Fribourg, Chemin du Musée 9, 1700 Fribourg, Switzerland

GRAPHICAL ABSTRACT

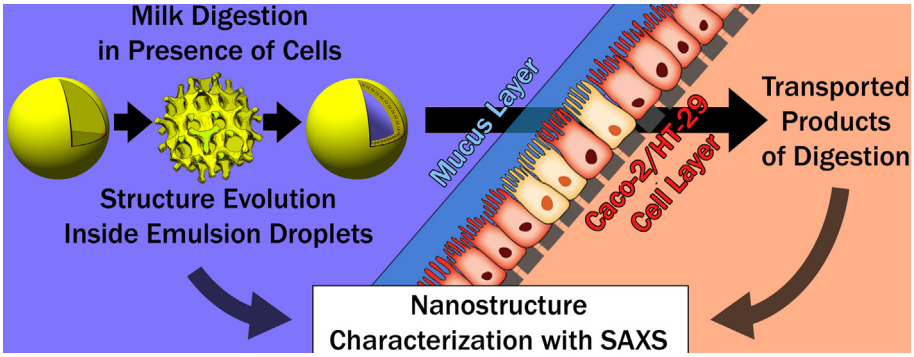

ARTICLE INFO

Article history:
Received 23 February 2020
Revised 15 April 2020
Accepted 15 April 2020
Available online 18 April 2020

Keywords:
In vitro digestion
Food colloids
Self-assembly
Liquid crystals

ABSTRACT

Hypothesis: The development of advanced oral delivery systems for bioactive compounds requires the fundamental understanding of the digestion process within the gastrointestinal tract. Towards this goal, dynamic *in vitro* digestion models, capable of characterising the molecular as well as colloidal aspects of food, together with their biological interactions with relevant *in vitro* cell culture models, are essential.
Experiments: In this study, we demonstrate a novel digestion model that combines flow-through time resolved small angle X-ray scattering (SAXS) with an *in vitro* Caco-2/HT-29 cell co-culture model that also contained a mucus layer. This set-up allows the dynamic *in situ* characterisation of colloidal structures and their transport across a viable intestinal cell layer during simulated digestion.
Findings: An integrated online SAXS – *in vitro* cell co-culture model was developed and applied to study the digestion of nature's own emulsion, milk. The impact of the *in vitro* cell culture on the digestion-

Abbreviations: $CaCl_2$, calcium chloride; CO_2, carbon dioxide; CPP, critical packing parameter; DMDM, Dulbecco's Modified Eagle Medium; DSMZ, Leibniz Institute DSMZ – German Collection of Microorganisms and Cell Cultures; EDTA, ethylenediaminetetraacetic acid; EtOH, ethanol; FCS, fetal calf serum; FFAs, free fatty acids; GIT, gastrointestinal tract; HCl, hydrochloric acid; HTS, high throughput screening; MEM, minimum essential medium; MeOH, Methanol; MTT, Methylthiazolyldiphenyl-tetrazolium bromide; NaCl, sodium chloride; NaOH, sodium hydroxide; PBS, phosphate buffered saline; PET, polyethylene terephthalate; PFA, paraformaldehyde; SAXS, small angle X-ray scattering; SDS, sodium dodecyl sulfate; TEER, transepithelial electrical resistance; Tris Base, Tris (hydroxymethyl) aminomethane; USP, United States Pharmacopeia.

* Corresponding author at: University of Fribourg, Chemin du Musée 9, CH-1700 Fribourg, Switzerland.
E-mail address: stefan.salentinig@unifr.ch (S. Salentinig).

[1] Contributed equally.

https://doi.org/10.1016/j.jcis.2020.04.059
0021-9797/

Nanostructures
In situ SAXS
Caco-2/HT-29 co-culture
Milk
Mucus

triggered formation and evolution of highly ordered nanostructures in milk is demonstrated. Reported is also the crucial role of the mucus layer on top of the cell layer, protecting the cells from degradation by digestive juice components such as lipase. The novel model can open unique possibilities for the dynamic investigation of colloidal structure formation during lipid digestion and their effect on the uptake of bioactive molecules by the cells.

1. Introduction

There is a growing interest to understand, control, and manipulate the process of lipid digestion within the gastrointestinal tract (GIT) with functional food materials, particularly in regards to the development of emulsion-based systems for the delivery of hydrophobic and amphiphilic bioactive compounds [1–4]. However, the conduct of human or animal feeding studies to assess the impact of the wide range of food matrix components and their colloidal structures is unrealistic, not only due to ethical concerns but also for economical and practical reasons [5,6]. Further, a comprehensive understanding of the food-digestion interactions that ultimately allows the rational design of functional food materials requires a fundamental knowledge of the effect of individual digestion parameters such as bile salt concentration, pH, lipases, and interactions with mucus layer and cells, on the process. This is only possible with suitable *in vitro* models that offer the flexibility to modify selected parameters, within and even beyond the physiologically relevant range. To address this, numerous *in vitro* digestion models have been introduced over the last two decades, designed to mimic the *in vivo* situation of the GIT [6,7]. Most of the dynamic *in vitro* models were not successful in recreating the physiological conditions as the interaction and absorption of water, nutrients and metabolites could not be routinely simulated [6].

To date, the majority of published studies focused on the changes in the chemical composition during digestion using *in vitro* models that mimic gastric and small intestinal digestion consecutively, or *in vitro* cell culture models that evaluate epithelial permeability. The analysis of the digestion components and their interactions with epithelial cells was mostly carried out separately, by first performing the digestion *ex situ* in a bioreactor and subsequently introducing the digestion mixture to an *in vitro* intestinal cell model and/or porcine tissue grafts [8–11]. A predictive digestion model for real time evaluation of lipid digestions under physiologically relevant conditions in the presence of intestinal cells has only been recently described [12]. Contrary to the analytical chemistry aspects, the colloidal aspects of the digestion processes, such as self-assembled structure formation of food emulsions and amphiphilic digestion components from the micrometer down to the nanometer range, are mostly unstudied. These colloidal processes, that may play a crucial role in the digestion process, were first discovered during the *in vitro* digestion of olive oil emulsions using light microscopy [13]. The structures and their transformations inside a digesting triolein-in-water emulsion droplets were later demonstrated using an *in vitro* digestion model, without intestinal cells, that was coupled with *in situ* flow-through small angle X-ray scattering (SAXS) and further confirmed with cryogenic transmission electron microscopy [14]. The lipid digestion products, monoacylglycerols and free fatty acids (FFAs), self-assemble inside the oil droplet to form geometrically ordered lyotropic liquid crystalline structures. The type of formed nanostructure depends largely on the ratio between fatty acid / monoglyceride / diglyceride / triglyceride inside the emulsion droplets and this ratio is gradually changing during the course of digestion. The observed structures and their transformations in these self-assembled systems agree with predictions from the critical packing parameter (CPP) model (see the SI for definition) [15,16]. Bile salts, which are also part of the digestive juice, have been shown to actively participate in this self-assembly process through composition-dependent modification of the nanostructures [14,17]. Recently, lyotropic liquid crystalline structures together with vesicles and micelles were also detected during the *in vitro* digestion of bovine and human breast milk, and the triglyceride-based food product mayonnaise in a digestion model simulating the small intestine in absence of cells that was coupled with *in situ* SAXS [18–20].

The formation of nanostructured lipid emulsions during digestion has been recently discussed to influence the delivery of lipid nutrients, enzymatic lipolysis, and interactions of the digestion products with the mucus and epithelial cells in the small intestine [21]. Lipolysis is a process which occurs at the lipid water interface and, as a consequence, the large new lipid water interfaces generated during the digestion of emulsions can play a crucial role in this process and deserve to be analysed in *in vitro* digestion models [22]. Considering this knowledge gap, the studies of digestion processes could benefit from more sophisticated *in vitro* digestion models coupled with flow-through time-resolved online SAXS for the determination of nanostructures in real-time. Together with *in vitro* cell culture models that mimic the intestinal epithelium, such models would allow a systematic study of interactions between the digestion structures and components with the epithelium. These advanced models combining biophysical approaches with relevant cell culture models will eventually pave the way for a more detailed understanding of the digestion process that is necessary for the rational design of functional food- and drug delivery materials.

Overall, the challenge in simulating the lipid digestion lies in the complexity of the diverse processes occurring *in vivo.* The first step of any digestion in humans is the mouth, where the lipid droplets interact with the saliva, tongue, and oral cavity [5]. The mixture of the food matrix with saliva is then passed through the stomach where the emulsion droplets are further fragmented under the exposure to low pH conditions (typically around 2–3), salts, enzymes, and mechanical forces [5,14,23]. Upon leaving the gastric compartment and entering the intestine, the pH is increased to around 6–8, and enzymes such as pancreatic lipase and biologic surfactants such as bile salts and phospholipids are introduced [5,24]. These components are then responsible for the lipid digestion and absorption that occurs mainly in the small intestine [25]. Bile salts and phospholipids further help stabilize the emulsion droplets and optimize their surface for the adsorption of the surface active pancreatic lipase-colipase complex [26–30]. After adsorption, the pancreatic lipase stereospecifically hydrolyses the two outer ester bonds of the triglyceride oils (*sn-1* and *s-3)* inside the emulsion droplet, resulting in the generation of the *sn-2* monoglyceride and the corresponding FFAs [31]. These amphiphilic digestion products then form a range of self-assembled nanostructures, which may target interaction with the brush border of the intestinal epithelia cells where they are ultimately absorbed [26]. From there, the epithelia cells release the

long-chain lipids in the form of packed lipoproteins, also known as chylomicrons to the basolateral side, where they are transported via the lymphatic system to other tissues [32,33].

One of the most widely used experimental models to characterise the lipid digestion in the small intestine under simulated conditions is the pH-stat method [34–36]. In this cell-free and 'closed' method, the pH is kept constant by titrating the pH change that is caused by the release of FFAs during the hydrolysis of triglycerides with NaOH. The quantity of the released FFAs can then be estimated by the moles of NaOH required to maintain a constant pH [5,37]. However, this 'closed' model ignores the removal of the digestion products through absorption by the epithelial cells in the small intestine, along with all its consequences for the digestion reaction.

To the best of our knowledge, the nanostructure formation in food emulsions during their digestion has not yet been demonstrated in presence of *in vitro* intestinal cell models that closely mimic the *in vivo* situation in the small intestine, including the absorption and removal of digestion products. Such a model can lead to a more comprehensive understanding of the digestion-triggered nanostructure formation during lipid digestion, and the resulting implications on nutrient uptake and transport by the cells. It requires the integration of physiologically relevant cell culture models into the current pH-stat model that is then coupled with flow-through online SAXS. Here, the cell culture models should resemble the structure of the intestinal epithelium more closely than current Caco-2 models that lack the mucus, for instance with co-culture of Caco-2 and mucus secreting cells [38–41].

In this study a novel platform for the online investigation of colloidal structure formation during digestion in the presence of an *in vitro* co-culture Transwell® model containing a mucus layer was developed. This platform allows the simultaneous monitoring of nanostructures on both sides of the co-culture cell layer. Firstly, the viability of *in vitro* intestinal cell layer models in the presence of pancreatin extract and milk were studied. Secondly, the optimized cell culture model was coupled to a flow-through digestion model with the pH-stat and synchrotron SAXS to discover the effect of mucus, cells and product absorption on the *in situ* nanostructure formation during the digestion of nature's own emulsion, milk. Simultaneously, the other side of the cell layer is monitored for potential nanostructure formation by digestion products that were transported through the mucus layer and the cell layer.

2. Materials and methods

2.1. Materials

Pancreatin from porcine pancreas (8 × United States Pharmacopeia (USP) grade pancreatin activity) was purchased from Sigma Aldrich (St. Louis, MO, USA). It is a mixture of digestive enzymes produced by the exocrine cells of the porcine pancreas and contains enzymes such as pancreatic lipase, amylase, trypsin, ribonuclease, and protease. Acetic acid (purity ≥ 99.7%), Alcian Blue 8GX (dye content ≥ 45–65%), Chloroform (purity ≥ 99.8%), Crystal Violet (dye content ≥ 90%), hydrochloric acid (HCl, concentration = 3 7%), maleic acid (purity ≥ 98.0%), Nuclear Fast Red (for microscopy), paraformaldehyde (PFA, 95–100%), phosphate-buffered saline (PBS, sterile-filtered; pH = 7.4), sodium dodecyl sulphate solution (SDS, BioUltra, for molecular biology, 20% in H_2O), Thiazolyl blue tetrazolium bromide (MTT, purity = 98%), Tris Base/ Tris (hydroxymethyl) aminomethane (for fish-farming, pH 8.3; 93367), sodium chloride (NaCl) (≥99.5%) were purchased from Sigma Aldrich (Buchs, Switzerland). Calcium chloride ($CaCl_2$, p.a. grade, EMSURE®) was purchased from Merck (Darmstadt, Germany) and ethanol (EtOH, purity ≥ 99.8%) from Honeywell (Bucharest, Romania).

Standardized unskimmed milk with 3.5% milk fat was bought from a local shop (Switzerland). 0.2 M sodium hydroxide (NaOH, practical grade) and 0.2 M HCl from Sigma Aldrich (St. Louis, MO, USA) were used for pH adjustment. Ultra-pure water (R > 18 MΩ) was used for the preparation of all samples. The digestion buffer (pH 6.5) contained 50 mM maleic acid, 50 mM Tris Base, 5 mM $CaCl_2$ and 150 mM NaCl.

2.2. Cell culture

The human colorectal adenocarcinoma cell line Caco-2 was obtained from the German collection of microorganisms and cell cultures (DSMZ, Braunschweig, Germany). Cells were maintained in Minimum Essential Medium (MEM, Sigma, M2279) at a physiological pH of 7.4, supplemented with 10% fetal calf serum (FCS; F9665), 2 mM L-glutamine (G7513), 1% (v/v) penicillin, streptomycin, neomycin (P4083) (all from Sigma Aldrich, Buchs Switzerland), and 1% (v/v) non-essential amino acids (PAN, Aidenbach, Germany; P08-32100) (hereafter called "complete MEM") at 37 °C, 5% CO_2, and 95% humidity, hereafter called "standard growth conditions". Caco-2 cells were grown in 75 cm^2 cell culture flasks (TPP, Trasadingen, Switzerland) until reaching 80% confluence and subcultured using trypsin-ethylenediaminetetraacetic acid (EDTA) (Sigma Aldrich, T3924).

The human colon cell line HT29-MTX-E12 (hereafter called "HT-29″) was obtained from the European Collection of Authenticated Cell Cultures (ECACC, England). Cells were maintained in Dulbecco's Modified Eagle Medium (DMEM, obtained from Sigma, D5796) at pH 7.4, supplemented with 10% fetal calf serum (FCS), 2 mM L-glutamine, 1% (v/v) penicillin, streptomycin, neomycin (all from Sigma Aldrich, Buchs Switzerland), and 1% (v/v) non-essential amino acids (PAN, Aidenbach, Germany) (hereafter called "complete DMEM") at standard growth conditions. HT-29 cells were grown in 75 cm^2 cell culture flasks (TPP) until reaching 80% confluence and subcultured using trypsin-EDTA (Sigma).

2.3. Caco-2 monocultures

Caco-2 cells were initially used as an *in vitro* digestion model for the digestions experiments. To obtain a differentiated Caco-2 monolayer, cells were seeded at a concentration of 2 × 10^4 cells/mm^2 into the apical compartment of microporous polyester (PET) membrane inserts (Corning® high throughput screening (HTS) Transwell®-96 Tissue Culture Systems (pore size: 1 μm) (Corning, Kaiserslautern, Germany) or ThinCert™ Tissue Culture Inserts 6 Well Greiner Bio-One (pore size: 3 μm) (Greiner Bio-One, St. Gallen, Switzerland)). The basolateral compartment was filled with complete MEM and cells were allowed to differentiate under standard growth conditions for 18 days for the cell viability assessment and for 16 and 18 days for the SAXS experiments. Medium was changed every 48 h. All monoculture experiments, were conducted on Caco-2 cells in differentiated state.

2.4. Caco-2/HT-29 co-cultures

Intestinal co-cultures were based on the co-culturing of Caco-2 and HT-29 cells with a predefined seeding ratio of 75:25 to achieve a confluent mucus layer. An overall cell seeding concentration of 2×10^4 cells/mm^2 for the apical compartment of microporous membrane inserts (Corning® HTS Transwell®-96 Tissue Culture Systems (pore size: 3 μm) or Corning® 75 mm Transwell® Permeable Supports, (pore size: 3 μm)) was maintained (Corning, Kaiserslautern, Germany). The basolateral compartment was filled with complete DMEM and cells were allowed to differentiate under

standard growth conditions for 18 days for the cell viability assessment and for 16-18 days for the SAXS experiments. Medium was changed every 48 h. All co-culture experiments were conducted on differentiated Caco-2/HT-29 co-cultures.

2.5. Pancreatin extract preparation

For each experiment, 2 g of the porcine pancreatin were diluted in 5 ml of digestion buffer (50 mM maleic acid, 50 mM Tris Base, 5 mM $CaCl_2$ and 150 mM NaCl) and stirred for 20 min at 4 °C. The enzyme suspension was centrifuged at 4 °C at 4000 rpm for 15 min. The supernatant was recovered and kept on ice until further use in the viability or *in vitro* digestion studies. For the further dilutions for the toxicity experiments, the pH was adjusted to 6.5. For the milk digestion experiments, 1 ml of this pancreatin extract was added to 20 ml of 50% digestion buffer 50% milk suspension for the final concentration of 0.019 g/ml.

2.6. Cell viability (MTT assay)

The culture medium was removed from differentiated Caco-2 monocultures or differentiated Caco-2/HT-29 co-cultures in HTS 96-well inserts and Caco-2 monocultures were treated with concentrations of 0, 0.005, 0.01, 0.02, 0.04, 0.06 and 0.1 g/ml pancreatin extract and co-cultures with 0, 0.005 g/ml, 0.02 g/ml, 0.04 g/ml pancreatin extract for 30 min and 2 h on the apical side. The basolateral compartment was filled with complete cell culture medium made from phenol red free medium (Gibco). All samples without pancreatin extract received an equivalent volume of digestion buffer and milk and served as solvent control. The untreated sample received 100% complete cell culture medium and, to understand the impact of milk or digestion buffer on cell viability, additional controls were included with 100% milk or 100% digestion buffer. The MTT stock solution (5 mg/ml in PBS) was diluted freshly for every experiment in complete cell culture medium made from phenol red free medium. At 30 min and 2 h post-exposure, the wells were washed 2 times with warm PBS before 0.5 mg/ml MTT, in complete cell culture medium made from phenol red free medium, was added. On the apical side a volume of 75 µl/well was added and on the basolateral side it was 235 µl. The cells were incubated for 1.5 h at standard growth conditions. Afterwards, 37.5 µl of 10% SDS in 0.01 M HCl was added apically while the basal compartment was exchanged to an empty one. After efficient lysis of the cell layer the lysis solution was replaced into a new plate to measure the absorbance with a multi-well plate reader (Mithras2 LB943, Berthold Technologies) at 590 nm. Data shown represent the mean and corresponding standard deviations of two independent experiments with six technical replicates for the monoculture experiments and the co-culture experiments show three independent experiments with four technical replicates each.

Statistical analysis was conducted with GraphPad Prism 6 software using a one-way analysis of variance (ANOVA; 95% confidence interval) followed by the Dunnett's multiple comparisons test.

2.7. Measurement of transepithelial electrical resistance (TEER)

The differentiation process of the Caco-2 monolayers grown in 6-well inserts and the co-cultures grown in the 75 mm Transwell® inserts was controlled by TEER measurements after 7, 14, and 18 days using an Epithelia Voltohmmeter (EVOM) with sterilised STX2 electrodes (World precision, Instruments, Sarasota Florida, US). Only Caco-2 cell monolayers with TEER values higher than 750 Ω cm^2 and co-cultures with TEER values higher than 2800 Ω cm^2 were used for experiments.

2.8. Stainings

2.8.1. Crystal violet

For the 6-well inserts containing the Caco-2 monoculture, the apical treatment volumes were 4 ml/well and the cells were treated on the basal side in complete cell culture medium made from phenol red free medium.

After the experiment, the 6-well Transwell® inserts were fixed with 4% PFA for 1 h to preserve the cell layer. For long-term storage the cells were immersed in 50% EtOH and kept at 4 °C. The crystal violet staining was conducted after a protocol described by May et al. [42]. In brief, the samples were additionally fixed in 20% ice cold methanol (MeOH) for 5 min and stained with 0.5% crystal violet in 20% MeOH for 10 min, before they were washed and dried.

2.8.2. Alcian blue

For the investigation of the mucus layer, an alcian staining has been conducted. The 6-well Transwell® inserts were fixed for 2 h with modified Carnoy solution (60% EtOH, 30% chloroform; 10% acetic acid) to preserve the mucin layer. For long-term storage, the cells were immersed in 50% EtOH and kept at 4 °C. More detailed information can be found in the published staining protocol [43]. In brief, the samples were stained with alcian blue for 30 min before they were dehydrated and mounted.

2.9. Coupling synchrotron small angle X-ray scattering and pH-stat with the in vitro cell culture model

The nanostructure formation during the digestion of milk in a digestion model that couples the pH-stat method with an *in vitro* cell culture model was studied *in situ* using flow-through SAXS (Fig. 1). The digestion reaction was conducted in a large Transwell® insert with surface area of 75 cm^2 that was seeded with co-cultured Caco-2 and HT-29 cells at 37 °C. 20 ml of 1/1 vol/vol mixture of milk and digestion buffer was filled onto the apical side of the plate, onto the cell layer. The basolateral side of the Transwell® inserts received 60 ml complete cell culture medium, DMEM. The pH on the apical side was recorded with a LL Biotrode pH meter (Metrohm AG, Herisau, Switzerland) on a Titrando 906 titrator (pH-stat, Metrohm AG, Herisau, Switzerland). The pH-stat titrated the digestion mixture on the apical side with 0.5 M NaOH solution (Titrosol, Merck KGaA, Darmstadt, Germany) to maintain pH at defined values during the digestion reaction. The pH electrode and titrator tube were attached to a shaker plate (Heidolph Titramax 101, Schwabach, Germany), to gently stir the digestion mixture on top of the Transwell® insert at 300 rpm. The basolateral side of the Transwell® was mixed with a magnetic stirrer. To improve cell viability and mimic body temperature, the whole cell set up was placed in a 37 °C water bath.

For the *in situ* SAXS study of structure formation on both, the apical and basolateral site of the Transwell® insert, two flow-through borosilicate capillaries (1.5 mm thick, Hilgenberg GmbH, Malsfeld, Germany) were fixed on a movable sample stage in front of the synchrotron X-ray source. The digestion mixture and culture media from the apical and basolateral side of the cell monolayer, respectively, were circulated in separate tubing connected to separate capillaries. Polytetrafluoroethylene tubing (0.5 mm inner diameter, BOLA, Bohlender GmbH, Grünsfeld, Germany) and a peristaltic pump (Alitea MIDI-D U1, Alitea AB, Stockholm, Sweden) connected the two sides of the Transwell® and the flow-through capillaries. The flow rate was approximately 10 ml/min, to avoid beam damage. The digestion reaction was started with a syringe pump (neMesys, centoni GmbH, Korbußen, Germany) for remotely adding 1 ml of the prepared pancreatin extract with a speed of approximately 0.2 ml/s to the buffer/milk mixture on the apical side of the Transwell®.

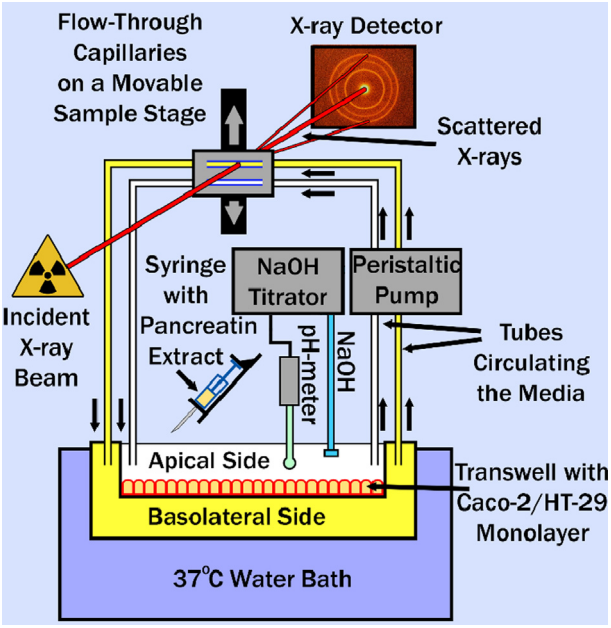

Fig. 1. Experimental setup used for the *in situ* study of the digestion of milk in the presence of a Caco-2/HT-29 co-culture. Nanostructure formation was simultaneously monitored with online SAXS on the apical and basolateral side of the cell layer.

Online SAXS patterns of the two capillaries were collected during the lipolysis by frequently moving the capillaries in and out of the X-ray beam by using the sample stage. The measurements were performed on the cSAXS beamline at the Swiss Light Source, Paul Scherrer Institute (PSI, Villigen, Switzerland) with an X-ray beam having a wavelength of 1.0 Å at X-ray energy of 12.4 keV. With the sample-to-detector distance of 2157.7 mm, the scattering vector magnitude, q, covered the range of 0.06–5.0 nm^{-1} ($q = 4\pi/\lambda \sin\theta$, where λ is the wavelength and 2θ is the scattering angle). Beamsize was 100 × 100 μm^2. The *in situ* SAXS patterns were acquired over at least 70 min of digestion with an exposure time of 1 s and a 9 s delay between the frames, using a Pliatus 2 M detector (in-house prototype) with an active area of 254 × 289 mm^2 and a pixel size of 172 × 172 μm^2. The two-dimensional (2D) scattering frames were radially integrated into 1D curves and plotted as a function of scattering intensity $I(q)$ vs q. Afterwards, the scattering from PBS was subtracted as background. For clarity, only one frame every minute of digestion is presented. Bragg peaks in the scattering curves were fitted by Lorentzian distributions to estimate their q-positions. The lattice parameters of inverse cubic (a_{Im3m}) and inverse hexagonal (a_{H_2}), as well as the d-spacing of lamellar phase were calculated from the q-values of the respective Bragg reflections as described below:

$$a_{H_2} = \frac{4\pi}{q_{hkl}\sqrt{3}}\sqrt{h^2 + hk + k^2} \quad (1)$$

$$a_{Im3m} = \frac{2\pi}{q_{hkl}}\sqrt{h^2 + k^2 + l^2} \quad (2)$$

$$d = \frac{2\pi h}{q_h} \quad (3)$$

where q_{hkl} is the q-value of the Bragg peak corresponding to the reflection with the h, k, and l Miller indices, and q_h is the q-value of the h-th order Bragg peak of the lamellar phase.

3. Results and discussion

3.1. Design and optimisation of the in vitro cell culture model

The most widely used intestinal *in vitro* cell culture model is differentiated Caco-2 monolayers which represents the main epithelial cell type of the intestinal barrier [44,45]. When cultivated on Transwell® inserts, these cells become highly polarized and express an extensive microvilli brush border similar to the physiological situation making them more resistant to toxicity from nanomaterials [45–47] However, differentiated Caco-2 monolayers do not express a mucus layer, an additional protective physical-chemical barrier of the intestine [45]. Treatment of Caco-2 cell monolayers on 6-well Transwell® inserts with 50% milk/ 50% digestion buffer or 100% digestion buffer for 2 h did not show any considerable cell death as visualized by the presence of an almost intact monolayer (Fig. 2A and B). However, incubation with 0.04 g/ml pancreatin extract in 100% digestion buffer and 50% milk/ 50% digestion buffer mixture resulted in the loss of large parts of the cell layer (Fig. 2C, D), where in the latter case the digestion mixture required for emulsion digestion experiments resulted in the loss of approximately 45–50% of coverage. In this context, the intestinal digestion of milk takes at least 30 min [18] and mice experiments have shown that the *in vivo* uptake of FFAs takes between 30 and 60 min [48].

Therefore, a cell layer that survives at least 30 min in presence of the pancreatin extract would be desirable to investigate colloidal structures during milk digestion and the impact of the presence of the cell culture on the structure formation. Whereas the presence of digestion buffer and milk does not impact on the Caco-2 cells viability in the first 30 min (Fig. 2E), the presence of pancreatin extract led to significant cell death (Fig. 2F). Even at lower pancreatin concentrations of 0.02 g/ml, less than 75% of the Caco-2 cells were viable after 30 min (Fig. 2F). It appeared that the pancreatin extract resulted in the digestion of the differentiated Caco-2 monolayer after 30 min at 37 °C.

To prevent digestion of the enterocyte cell layer and ensure an adequate lipid uptake, a more sophisticated co-culture model with enterocyte (Caco-2) and mucus-producing goblet cells (HT-29-MTX) was investigated. The co-cultivation of Caco-2 and HT-29 cells provides adequate mucus coverage for the cell monolayer as previously reported in the literature [39,49–54]. Staining of the co-culture used in this study with alcian blue confirmed the formation of a mucus layer (Fig. S1A). Cell viability of the co-culture after 30 min and 2 h of incubation with pancreatin extract was determined using the MTT assay. Incubation of the co-culture in cell culture medium, 50% milk/ 50% digestion buffer, 100% milk or 100% digestion buffer induced no considerable changes in cell viability up to the 2 h of cultivation (Fig. 3A, B). After 30 min as well as 2 h incubation, the viability after treatment with pancreatin extract (0–0.1 g/ml) remained above 80% compared to the solvent control, except for the highest pancreatin extract concentration (0.1 g/ml) at 2 h of cultivation (Fig. 3C). The improved viability of Caco-2/HT-29 co-cultures compared to Caco-2 monocultures indicates that the mucus layer formed a protective barrier against the digestive activity of the pancreatin extract components. The high standard deviation between the different experiments at both time points could be due to differences in the thickness of the mucus layer produced by individual cultures. A thinner mucus layer could be less efficient in preventing digestion of the cells. The alcian blue staining showed that the height of the mucus layer *in vitro* (few tens of micrometers) was not comparable to the 123 μm high mucus layer found in the rat jejunum [55,56]. Nevertheless, the *in vitro* formed mucus layer was sufficient to protect cells for at least 2 h from the cytotoxic effects of the pancreatin extract and

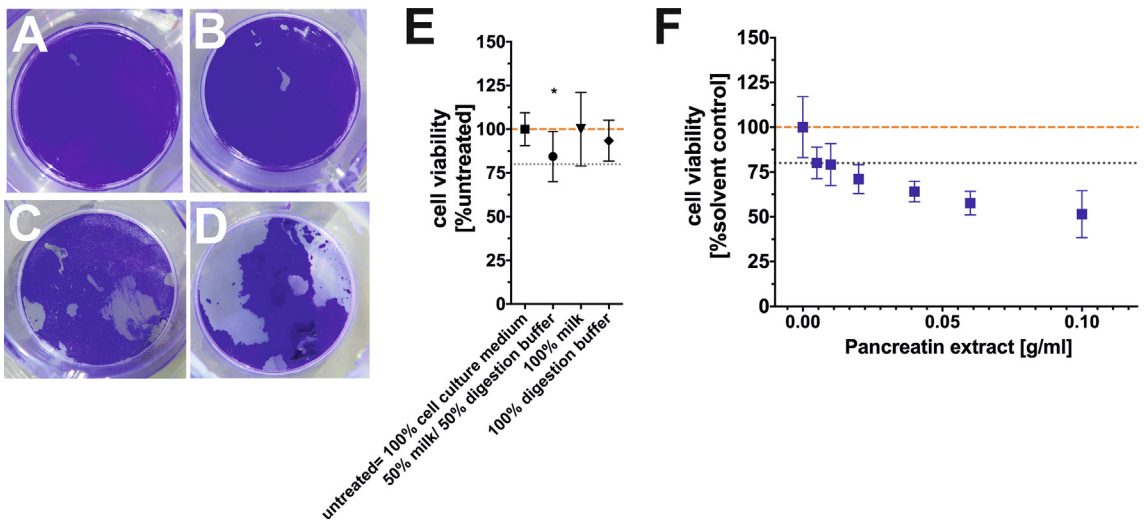

Fig. 2. Assessment of the cell viability of differentiated Caco-2 monocultures. Cristal violet staining shows the intactness of the Caco-2 cell monolayer after 2 h of treatment with (A) 50% milk/ 50% digestion buffer (B) 100% digestion buffer (C) 0.04 g/ml pancreatin extract in 100% digestion buffer (D) 0.04 g/ml pancreatin extract in 50% milk/ 50% digestion buffer. Cell viability was assessed with the MTT assay after 0.5 h of cultivation in (E) different buffers and (F) in the presence of increasing concentrations of pancreatin extract in 50% milk/ 50% digestion buffer, which also acts as the solvent control in this experiment. Mean values and corresponding standard deviations from two independent experiments are shown, with six technical replicates each. The mean values of the untreated control samples (E) or of the solvent controls (F) are indicated by a dashed orange line in each graph. Grey dotted lines (E, F) correspond to 80% viability. (One-Way ANOVA with Dunnett Post Test: $p \leq 0.05$).

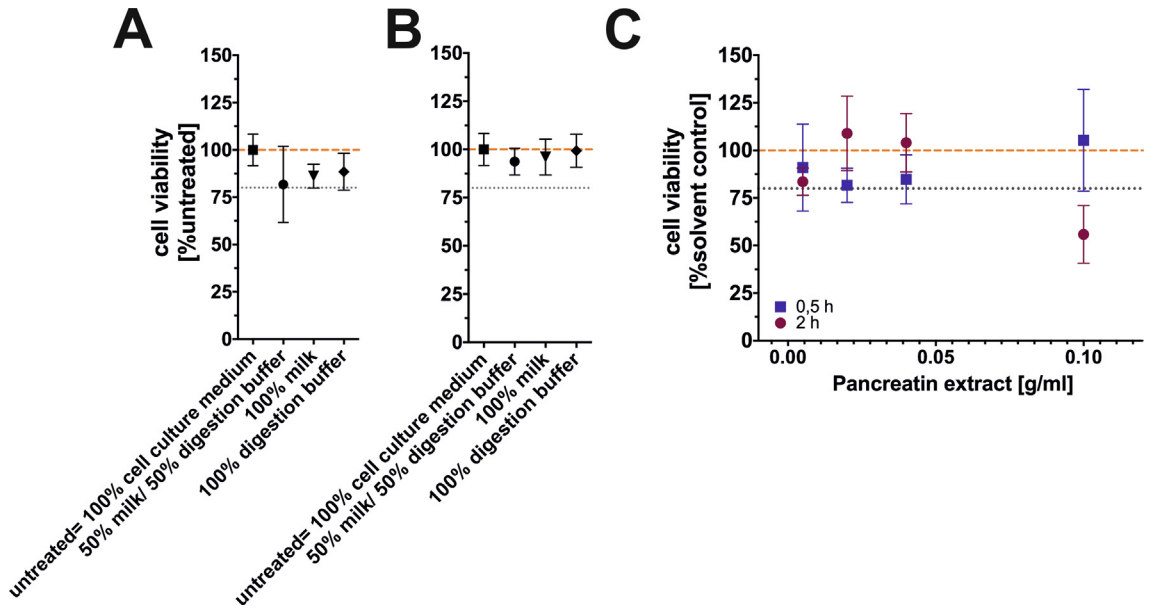

Fig. 3. Assessment of the cell viability of Caco-2/HT-29 co-cultures. Cell viability was assessed by MTT assay after (A) 0.5 h or (B) 2 h of cultivation in different buffers and in the presence of (C) increasing concentrations of pancreatin extract containing lipase in 50% milk/ 50% digestion buffer, which also acts as the solvent control in this experiment. Mean values and corresponding standard deviations of three independent experiments with four technical replicates each are shown. The mean values of the untreated control samples (A, B) or the solvent controls (C) are indicated by a dashed orange line in each graph. Grey dotted lines (A-C) correspond to 80% viability.

thus, Caco-2/HT-29 co-cultures could be used for digestion experiments.

The group of Lv et al. [11] did overcome lipase digestion of the cell layer by performing the digestion reaction separate from the *in vitro* intestinal model and sequentially transferring the digestive residues to the cell surface after a heat inactivation step. However, this has the disadvantage that a potential impact of the cells on the formation and evolution of structures during digestion could not be investigated. Keemink and Bergström [57] worked with immobilized lipase form Candida antarctica to prevent the Caco-2 cell layer from getting in contact with the lipase and suffer digestion. However, the use of lipase immobilized on surfaces limits the contact of the enzyme with the emulsion droplets, thereby compromising the reaction [58]. In contrast, our newly developed digestion platform allows for the direct investigation of milk digestion in the presence of a viable intestinal co-culture model simulating the human intestine by the usage of pancreatin extract, which includes a complex mixture of digestive enzymes [5]. Additional refinements of the digestion platform could be achieved by further optimizing the digestion buffer to also include biological surfactant (e.g. bile salts and phospholipids) or mimic physiological osmolarity [5]. Since *in vivo* relevant values of bile salts and osmolarity can be cytotoxic to intestinal cells *in vitro* [59], similar cell compatibility assays as performed in this study would be needed.

McClements and Li proposed, based on data by des Rieux et al. [60], that lipid droplets may be trapped by the mucins of the mucus layer [5]. To verify that the mucus layer does not act as a barrier in preventing the lipid transport by the intestinal co-cultures, a lipid uptake assay with a fluorescent model fatty acid analog was performed. Sufficient transport across the mucus and subsequent cellular uptake of the lipid by the cell layer was observed within 1 h, as seen from the fluorescence measurements presented in Fig. S1B. The observed permeability of the mucus layer to the fatty acid molecules further confirms the suitability of the co-culture for the investigation of *in situ* digestion studies with this model.

3.2. Nanostructure formation during milk digestion in the presence of Caco-2/HT-29 cell co-cultures

Fig. 4A shows the evolution of the SAXS patterns collected during the lipolysis of the 50% milk/ 50% digestion buffer mixture on the apical side of the Caco-2/HT-29 co-culture. Prior to the addition of the pancreatin extract on the apical side, the milk mixture displayed a SAXS curve with a low-q upturn in intensity ($\sim q^{-4}$ dependence of $I(q)$ in the low-q range, see Fig. S2) characteristic of scattering from particles with dimensions larger than the resolution of the SAXS setup, such as large emulsion droplets. Two broad correlation peaks at $q \approx 0.7$ and 1.5 nm^{-1} were observed in the same curve (Fig. 5), indicating presence of coexisting smaller nano-objects. The addition of the pancreatin extract containing lipase was immediately followed by NaOH titration (Fig. S3). Within 4 min of addition, a broad correlation peak with a maximum around q = 1.36 nm^{-1} was observed, indicating the formation of inverse micellar (L_2) phase inside the emulsion droplets (emulsified microemulsions, EME) (Fig. 5). Additionally, two weaker correlation peaks were also observed at around $q \approx 2.7$ nm^{-1} and 4.1 nm^{-1}. Together with the peak at q = 1.36 nm^{-1}, these three equidistant reflections correspond to the scattering from lamellar phase with the interlamellar distance, d, of 4.6 nm. The intensity of these reflections increased over the course of the lipolysis, whereas no discernible change in peak positions was detected (Fig. 5). About 7 min after the start of lipolysis, Bragg reflections with relative spacing of $1 : \sqrt{3} : \sqrt{4}$ were observed, indicating the formation of inverse hexagonal (H_2) phase inside the milk emulsion droplets (Fig. 4A). The H_2 phase peaks reached the highest intensity after around 10 min of digestion and were no longer present after 18 min of digestion (Fig. 5). The calculated lattice parameter a_{H_2} gradually increased from 6.2 to 6.4 nm (7 to 17 min) as the digestion progressed after the addition of lipase. Additionally, Bragg reflections with relative spacing of $\sqrt{2} : \sqrt{4} : \sqrt{6}$ were detected in the scattering curves 11 to 46 min after the addition of lipase, indicating the formation of a coexisting inverse bicontinuous cubic phase with *Im3m* symmetry inside the oil droplets (Fig. 5). The calculated a_{Im3m} was observed to gradually increase from 17.8 to 22.6 nm. The evolution of the lattice parameters throughout the *in vitro* digestion is summarized in Fig. S4. After 47 min and until the end of the *in vitro* digestion, the SAXS curve showed only the 3 equidistant peaks (Fig. 5) and a q^{-2} dependence of $I(q)$ in the low-q range (Fig. S2), indicating the presence of mostly dispersed lamellar structures i.e. in the form of single- and multilamellar vesicles. It is worth highlighting that similar colloidal transformations, leading to hierarchically organised dispersions that may function as carriers for poorly water-soluble bioactive molecules, were previously reported during the digestion of dairy and human breast milk in absence of cells [18,19]. The pH on the apical side of the cell monolayer was observed to gradually increase above 6.5 after around 37 min of digestion (Fig. S4). Even though no NaOH was titrated after 37 min of digestion (Fig. S3), the pH reached 6.8 after 70 min of digestion. The increase in the pH of the digestion mixture in the apical compartment could potentially be caused by two factors: the response of the cell layer, or compromised agitation of the milk buffer mixture causing over-titration with NaOH in certain regions of the digestion mixture.

The SAXS curves of the complete culture medium on the basolateral side of the cell layer during milk lipolysis are presented in Fig. 4B. The shape of the scattering curves with significant scattering intensity below q of around 1.0 nm^{-1} is most likely attributed to the proteins and protein aggregates in the complete culture medium. The SAXS curves don't appear to change throughout the duration of the *in vitro* lipolysis experiment (see Fig. 4B). However, transport and release of digestion products to the basolateral compartment in the form of packed lipoproteins (in the size range between tens and hundreds of nanometres [61]) cannot be excluded as the scattering of these structures would overlap with that of our culture medium. Hence, an optimized cell culture medium with reduced background scattering, and the integration of *in situ* light scattering methods into the basolateral side of the digestion model would be recommended for future experiments to further investigate these systems. In addition, the absence of scattering from lamellar or non-lamellar liquid crystalline structures indicates that no mixing occurred between the solutions on either side of the cell layer. This result confirms that the cell layer remained intact throughout the experiment and agrees with our previous viability measurements which did not show considerable cell death during the digestion.

The SAXS curves collected for the control lipolysis experiment at pH 6.5 without the presence of the *in vitro* cell culture model, are presented in Fig. 6. Before the addition of pancreatin extract, milk displayed a scattering pattern similar to the one in the presence of the cells (Fig. S5). Notably, the observed broad correlation peaks at $q \approx 0.7$ and 1.5 nm^{-1} were less pronounced in the absence of cells, potentially due to absence of mucus or other cell secretions. Upon the introduction of pancreatin extract, the correlation peak of the emulsified L_2 phase and the Bragg reflections of the lamellar phase were observed within 2 min (Fig. 6B). The calculated interlamellar distance was 4.6 nm throughout the experiment, similar to the *in vitro* digestion in the presence of cells. Already 5 min after pancreatin addition, Bragg reflections corresponding to the dispersed H_2 phase witha_{H_2} = 6.2 nm were observed. Growing in intensity and reaching maximum after 6 min (Fig. 6B), the H_2 phase Bragg peaks were observed to also shift to lower q values over time, indicating an increase in a_{H_2} to 6.4 nm after 7 min of lipolysis, but were no longer detected after 8 mins. Similar to the digestion experiment in the presence of cells, the Bragg peaks of the dispersed *Im3m* phase were also observed in the control digestion experiment without cells. Initially appearing 6 min after lipase addition, the intensity of the *Im3m* Bragg peaks was steadily increasing over the course of lipolysis (Fig. 6A). Starting with a_{Im3m} = 18.1 nm after 6 min, the dispersed *Im3m* phase was initially observed to gradually swell up to a_{Im3m} = 21.1 nm at 15 min of digestion. After 15 min, the cubic structure was observed to gradually shrink as the digestion progressed, reaching a_{Im3m} = 17.4 nm after 105 min of digestion. Furthermore, about 55 min after the digestion process began, the Bragg peaks of the dispersed H_2 phase were once again observed and continued to grow in intensity (Fig. 6B). The calculated a_{H_2} slightly decreased from 6.7 nm at 55 min to 6.6 nm at 105 min. The nanostructural changes over the course of lipolysis in the control experiment without cells at pH 6.5 are summarized in Fig. S6. The majority of the lipolysis (>70%) occurred in the first 8 min of the reaction, as evident from the amount of NaOH titrated (Fig. S3) and the temporary decrease in the pH of the dispersion to 6.3 (Fig. S6) due to

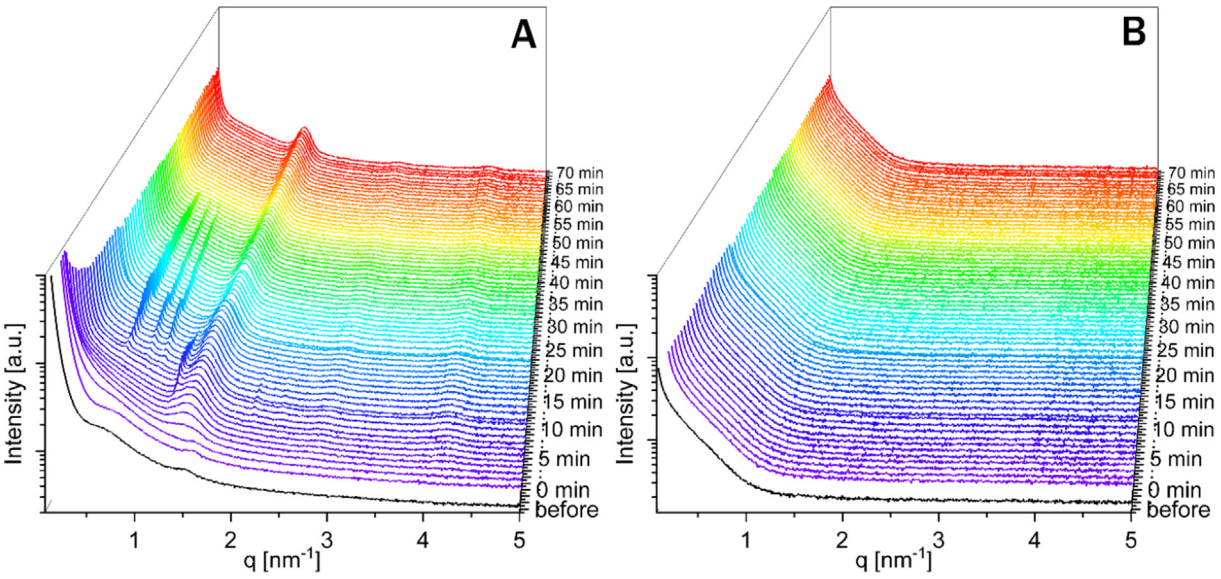

Fig. 4. Online SAXS measurements of milk digestion in the new digestion setup in the presence of Caco-2/HT-29 co-cultures at pH = 6.5. SAXS curves collected from the (A) apical and (B) basolateral side of the Caco-2/HT-29 co-cultures during *in vitro* digestion. Pancreatin extract containing the lipase was added to a 50% milk / 50% digestion buffer mixture on the apical side of the cell layer, while the basolateral side contained complete cell culture medium.

the rapid release of FFAs. It should also be noted that the nanostructural changes in the first 5–10 min of the digestion, including the appearance of H_2 phase, may also be impacted by this pH decrease. After 6 min equilibration, the pH was maintained at 6.5 as the digestion mixture could be more efficiently stirred in the absence of cells.

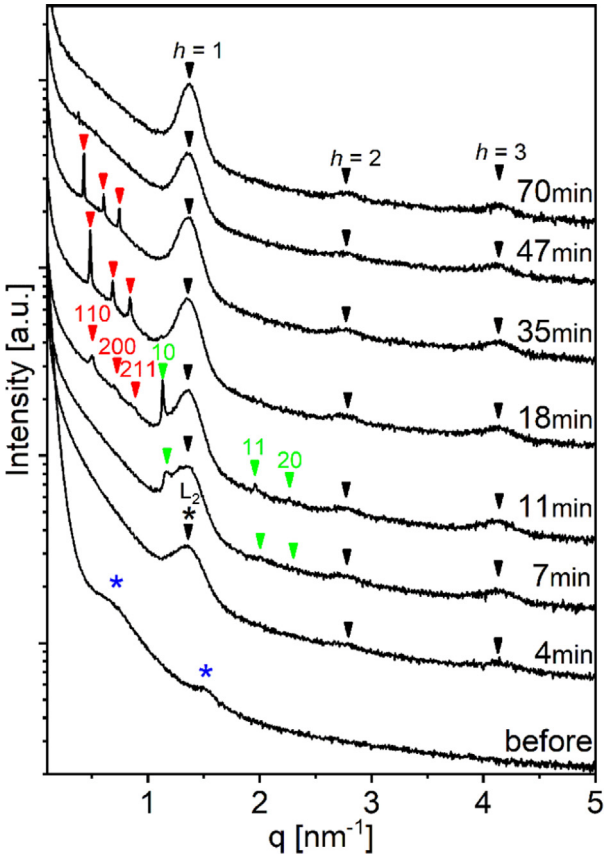

Fig. 5. SAXS curves collected from the milk mixture on the apical side of the Caco-2/HT-29 co-culture. The SAXS curves before addition of pancreatin extract, and at selected time points after the addition are shown, highlighting the assignment of self-assembled nanostructures. The first three peaks of the *Im3m, H_2, and L_α* phases are marked with red, green, and black arrows, respectively, and indexed with their corresponding Miller indices. Blue and black asterisks indicate the broad correlation peaks corresponding to coexisting nanoobjects and L_2 phase, respectively.

To evaluate the effect of pH on the self-assembled nanostructures during milk digestion, a control experiment without cells was also performed at the elevated pH of 7.0 (Fig. 7). Similar to the previous observations for this reaction at pH 6.5, the SAXS curves for the digestion performed at pH 7.0 demonstrated the presence of large emulsion droplets coexisting with nanosized objects (i.e. proteins) before the addition of pancreatin extract and indicated nanostructural transitions to the emulsified L_2 and lamellar phases within just 2 min after addition of the pancreatin extract. Bragg peaks indicative for the dispersed H_2 phase are briefly observed after 3–5 min of digestion, with the calculated a_{H_2} slightly increasing from 6.3 to 6.4 nm over the duration. The formation of the H_2 phase inside the milk emulsion droplet may be influenced by the temporary fluctuations in the measured pH within the first 6 min of this digestion experiment (Fig. S7), within which period the majority (>60%) of FFAs were cleaved from the triglycerides (Fig. S3). Only the Bragg reflections of the lamellar phase were observed after the 6 min of lipolysis at pH 7.0. It should be noted that the rate of digestion was similar at both pH 6.5 and 7.0 (Fig. S3). The formation of predominantly flat lipid-water interfaces of the lamellar phase during milk digestion at pH 7.0 and presence of inverse-type non-lamellar phases such as H_2 and *Im3m* when digestion occurred at pH 6.5, was most likely attributed to the differences in the protonation state of the FFAs at different pH [62–64]. The SAXS curve observed after 55 min of digestion in the absence of cells at pH 7.0 is similar to the scattering pattern observed at the same time point in the digestion experiment in the presence of Caco-2/HT-29 cells (Fig. S5). Both SAXS patterns are characteristic for lamellar structures, as discussed above. However, the scattering intensities are lower for the system in the presence of the cells, most probably due to absorption of digestion products (Fig. S5).

The formation of the emulsified L_2, lamellar and dispersed H_2 phases within the first minutes of digestion was observed in all the experiments of this study. The dispersed *Im3m* structure was also observed in presence and absence of cells in the digestions at pH 6.5. These findings highlight that dispersed non-lamellar liquid crystalline structures are generated during the digestion of

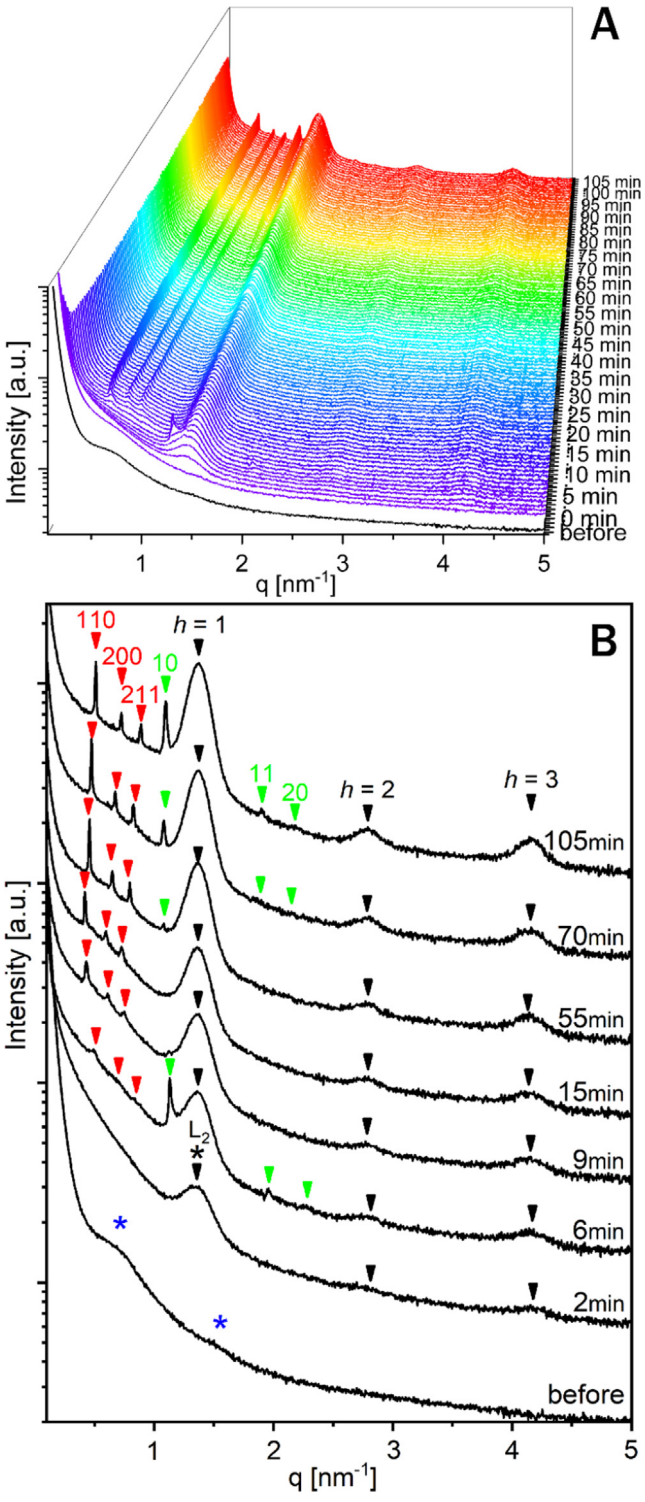

Fig. 6. SAXS curves for the digestion of milk solution with pancreatin extract at pH 6.5 in the absence of cells. Selected SAXS curves highlighting the self-assembled nanostructure assignment are presented in (B), with the first three peaks of the *Im3m*, H_2, *and* L_α phases marked with red, green, and black arrows, respectively, and indexed with their Miller indices. Blue and black asterisks indicate the broad correlation peaks corresponding to coexisting nano-objects and L_2 phase, respectively.

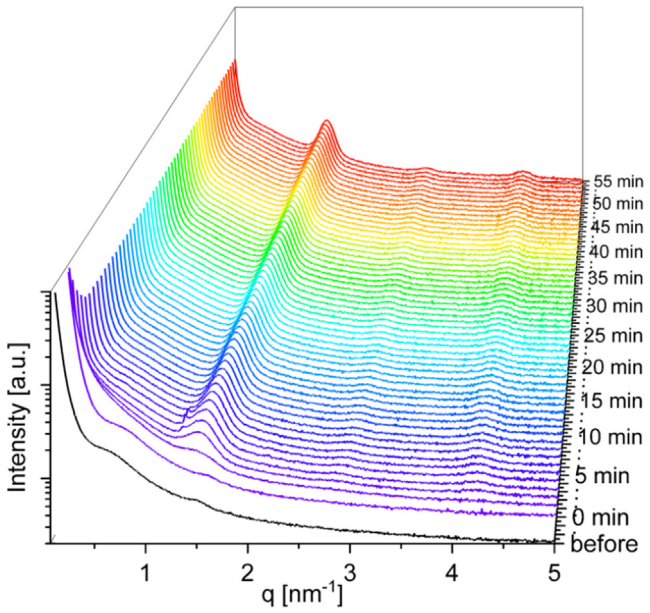

Fig. 7. SAXS curves for the digestion of milk mixture with pancreatin extract at pH 7.0 in the absence of cells.

milk in the presence of a mucus layer and cells that continuously absorb the digestion products. These structures may necessarily function as carriers for poorly-water soluble molecules, tailor the delivery of bioactive molecules and steer the interactions with the enzymes and eventually the mucus and cells in the small intestine.

It should be noted that the structure formation and phase transformation over the time of digestion was delayed by several minutes in the presence of the cell culture compared to the control experiment in absence of cells. Further, after 50 min of digestion, only lamellar structures such as vesicles were discovered in presence of cells at pH around 6.5. Contrary to that, dispersed non-lamellar structures were still coexisting with lamellar structures up to to more than 100 min of digestion in the absence of cells at the same pH value, in agreement with previous results on milk digestion [18]. This difference is most probably caused by the modified composition from absorption of digestion products into the cells. Further, a gradually lower scattering intensity was observed during digestion in the presence of the cells, relative to that in their absence (see Fig. S5). Over the course of digestion, this difference became more and more significant, which can be particularly noticed when looking at the first order reflections of the lamellar phase at q around 1.4 nm^{-1} in Fig. S5. The gradual removal of digestion products from the scattering volume by the cells may be the major reason for this. However, secondary effects such as slight variations in the solution pH or modified concentration of calcium ions in the presence of cells could also play a role. The presence of calcium ions has been reported to influence lipid digestion, and calcium is required for proper pancreatic lipase function [5,65–67]. It was also suggested by McClements and Li [5] that other natural components of the GIT, like mucins from the mucus or specific proteins, could be able to trap calcium ions, which could have influenced the lipase activity. It has been shown that in the presences of food, some components are able to bind calcium, like EDTA or alginate, and drastically reduce the lipase activity as a result [37]. Further investigations with optimized pH control and extended digestion duration are needed to gain a more precise understanding of the role that intestinal cells play in the colloidal transformations during the lipid digestion processes.

4. Conclusion and outlook

To the best of our knowledge, this is the first demonstration of a digestion platform with an integrated co-culture model for online

in situ investigation of lipid digestion and transport with synchrotron SAXS. Our findings further demonstrate that differentiated Caco-2 monolayers, commonly used for *in vitro* digestion studies, are not a suitable model for the *in situ* study of lipid digestion as these cells were found not to survive in presence of pancreatin extract. Instead, a co-culture model of Caco-2/HT-29-MTX cells [38,39,49,51], that additionally forms a protective mucus layer on top of the cells, has been employed and demonstrated to retain cell viability for more than 1 h of simulated digestion. The new platform was successfully applied to study the digestion of bovine milk. The formation and transformation of highly geometrically organized nanostructures in the lipid phase of the milk emulsion droplets during their digestion was observed for the first time in the presence of the co-culture with mucus and cell layer. These structures may tailor the digestion process and act as carriers for poorly water-soluble milk components. The results from the new co-culture model reveal differences in the evolution of lipid nanostructures throughout the digestion experiments in the presence or in the absence of cells. Our results indicate that this was caused by the modified composition in the digestive fluid through absorption of digestion products into the cells. For future studies, additional analytical methods to monitor the composition and the transport of lipids and co-administered nutrients simultaneously with nanostructure formation can be integrated on the apical and basolateral side of the cell layer in this digestion model. The new model from this study may ultimately allow the simultaneous research of the molecular as well as the colloidal length scale changes together with the biological functions *in situ* during the digestion in future studies. This fundamental knowledge can then guide the rational design of functional food products and delivery systems for hydrophobic and amphiphilic bioactive molecules including nutrients and drugs [68–70].

Credit authorship contribution statement

Claudia Hempt: Investigation, Validation, Formal analysis, Visualization, Writing - original draft. **Mark Gontsarik:** Investigation, Formal analysis, Visualization, Writing - original draft. **Tina Buerki-Thurnherr:** Supervision, Writing - review & editing. **Cordula Hirsch:** Methodology, Supervision, Writing - review & editing. **Stefan Salentinig:** Conceptualization, Funding acquisition, Methodology, Supervision, Writing - review & editing.

Declaration of Competing Interest

The authors declare that they have no known competing financial interests or personal relationships that could have appeared to influence the work reported in this paper.

Acknowledgements

The authors thank Dr. Philipp Berger (PSI, Villigen, Switzerland) for providing access to the cell culture facilities. The authors also thank the beamline scientists Dr. Ana Diaz and Dr. Manuel Guizar Sicairos for the technical support at the cSAXS beamline (PSI, Villigen, Switzerland).

Funding

This work benefitted from support from the Swiss National Science Foundation through the National Center of Competence in Research Bio-Inspired Materials. Hempt C. PhD project is funded by Evonik Industries and the NanoScreen Materials Challenge co-funded by the Competence Centre for Materials Science and Technology (CCMX).

Appendix A. Supplementary material

Supplementary data to this article can be found online at https://doi.org/10.1016/j.jcis.2020.04.059.

References

[1] Y. Pafumi, D. Lairon, P.L. de la Porte, C. Juhel, J. Storch, M. Hamosh, M. Armand, Mechanisms of Inhibition of Triacylglycerol Hydrolysis by Human Gastric Lipase, J. Biol. Chem. 277 (2002) 28070–28079, https://doi.org/10.1074/jbc.M202839200.
[2] C.J.H. Porter, N.L. Trevaskis, W.N. Charman, Lipids and lipid-based formulations: optimizing the oral delivery of lipophilic drugs, Nat. Rev. Drug Discov. 6 (2007) 231–248, https://doi.org/10.1038/nrd2197.
[3] C.J.H. Porter, K.M. Wasan, P. Constantinides, Lipid-based systems for the enhanced delivery of poorly water soluble drugs, Adv. Drug Deliv. Rev. 60 (2008) 615–616, https://doi.org/10.1016/j.addr.2007.10.009.
[4] D.J. McClements, E.A. Decker, Y. Park, J. Weiss, Designing food structure to control stability, digestion, release and absorption of lipophilic food components, Food Biophys. 3 (2008) 219–228, https://doi.org/10.1007/s11483-008-9070-y.
[5] D.J. McClements, Y. Li, Review of in vitro digestion models for rapid screening of emulsion-based systems, Food Funct. 1 (2010) 32–59, https://doi.org/10.1039/c0fo00111b.
[6] D. Dupont, M. Alric, S. Blanquet-Diot, G. Bornhorst, C. Cueva, A. Deglaire, S. Denis, M. Ferrua, R. Havenaar, J. Lelieveld, A.R. Mackie, M. Marzorati, O. Menard, M. Minekus, B. Miralles, I. Recio, P. Van den Abbeele, Can dynamic *in vitro* digestion systems mimic the physiological reality?, Crit. Rev. Food Sci. Nutr. 59 (2019) 1546–1562, https://doi.org/10.1080/10408398.2017.1421900.
[7] A. Brodkorb, L. Egger, M. Alminger, P. Alvito, R. Assunção, S. Ballance, T. Bohn, C. Bourlieu-Lacanal, R. Boutrou, F. Carrière, A. Clemente, M. Corredig, D. Dupont, C. Dufour, C. Edwards, M. Golding, S. Karakaya, B. Kirkhus, S. Le Feunteun, U. Lesmes, A. Macierzanka, A.R. Mackie, C. Martins, S. Marze, D.J. McClements, O. Ménard, M. Minekus, R. Portmann, C.N. Santos, I. Souchon, R.P. Singh, G.E. Vegarud, M.S.J. Wickham, W. Weitschies, I. Recio, INFOGEST static in vitro simulation of gastrointestinal food digestion, Nat. Protoc. 14 (2019) 991–1014, https://doi.org/10.1038/s41596-018-0119-1.
[8] E. Déat, S. Blanquet-Diot, J.-F. Jarrige, S. Denis, E. Beyssac, M. Alric, Combining the dynamic TNO-gastrointestinal tract system with a Caco-2 cell culture model: application to the assessment of lycopene and alpha-tocopherol bioavailability from a whole food, J. Agric. Food Chem. 57 (2009) 11314–11320, https://doi.org/10.1021/jf902392a.
[9] A.-K. Haraldsson, L. Rimsten, M. Alminger, R. Andersson, P. Åman, A.-S. Sandberg, Digestion of barley malt porridges in a gastrointestinal model: Iron dialysability, iron uptake by Caco-2 cells and degradation of β-glucan, J. Cereal Sci. 42 (2005) 243–254, https://doi.org/10.1016/j.jcs.2005.04.002.
[10] J. Westerhout, E. van de Steeg, D. Grossouw, E.E. Zeijdner, C.A.M. Krul, M. Verwei, H.M. Wortelboer, A new approach to predict human intestinal absorption using porcine intestinal tissue and biorelevant matrices, Eur. J. Pharm. Sci. 63 (2014) 167–177, https://doi.org/10.1016/j.ejps.2014.07.003.
[11] Q. Lv, Q. He, Y. Wu, X. Chen, Y. Ning, Y. Chen, Investigating the bioaccessibility and bioavailability of cadmium in a cooked rice food matrix by using an 11-day rapid Caco-2/HT-29 co-culture cell model combined with an in vitro digestion model, Biol. Trace Elem. Res. 190 (2018) 336–348, https://doi.org/10.1007/s12011-018-1554-0.
[12] J. Keemink, E. Mårtensson, C.A.S. Bergström, Lipolysis-permeation setup for simultaneous study of digestion and absorption in vitro, Mol. Pharm. 16 (2019) 921–930, https://doi.org/10.1021/acs.molpharmaceut.8b00811.
[13] J.S. Patton, M.C. Carey, Watching fat digestion, Science (80-.) 204 (4389) (1979) 145–148, https://doi.org/10.1126/science.432636.
[14] S. Salentinig, L. Sagalowicz, M.E. Leser, C. Tedeschi, O. Glatter, Transitions in the internal structure of lipid droplets during fat digestion, Soft Matter. 7 (2011) 650–661, https://doi.org/10.1039/C0SM00491J.
[15] J.N. Israelachvili, D.J. Mitchell, B.W. Ninham, Theory of self-assembly of hydrocarbon amphiphiles into micelles and bilayers, J. Chem. Soc. Faraday Trans. 2 (72) (1976) 1525, https://doi.org/10.1039/f29767201525.
[16] J.N. Israelachvili, D.J. Mitchell, B.W. Ninham, Theory of self-assembly of lipid bilayers and vesicles, Biochim. Biophys. Acta - Biomembr. 470 (1977) 185–201, https://doi.org/10.1016/0005-2736(77)90099-2.
[17] M.A. Long, E.W. Kaler, S.P. Lee, Structural characterization of the micelle-vesicle transition in lecithin-bile salt solutions, Biophys. J. (1994), https://doi.org/10.1016/S0006-3495(94)80647-2.
[18] S. Salentinig, S. Phan, J. Khan, A. Hawley, B.J. Boyd, Formation of Highly Organized Nanostructures during the Digestion of Milk, ACS Nano. 7 (2013) 10904–10911, https://doi.org/10.1021/nn405123j.
[19] S. Salentinig, S. Phan, A. Hawley, B.J. Boyd, Self-assembly structure formation during the digestion of human breast milk, Angew. Chemie Int. Ed. 54 (2015) 1600–1603, https://doi.org/10.1002/anie.201408320.
[20] S. Salentinig, H. Amenitsch, A. Yaghmur, In situ monitoring of nanostructure formation during the digestion of mayonnaise, ACS Omega (2017), https://doi.org/10.1021/acsomega.7b00153.
[21] S. Salentinig, Supramolecular structures in lipid digestion and implications for functional food delivery, Curr. Opin. Colloid Interface Sci. 39 (2019) 190–201, https://doi.org/10.1016/j.cocis.2019.02.002.

[22] T. Bohn, F. Carriere, L. Day, A. Deglaire, L. Egger, D. Freitas, M. Golding, S. Le Feunteun, A. Macierzanka, O. Menard, B. Miralles, A. Moscovici, R. Portmann, I. Recio, D. Rémond, V. Santé-Lhoutelier, T.J. Wooster, U. Lesmes, A.R. Mackie, D. Dupont, Correlation between in vitro and in vivo data on food digestion. What can we predict with static in vitro digestion models?, Crit. Rev. Food Sci. Nutr. 58 (2018) 2239–2261, https://doi.org/10.1080/10408398.2017.1315362.
[23] N. Scheuble, A. Iles, R.C.R. Wootton, E.J. Windhab, P. Fischer, K.S. Elvira, Microfluidic technique for the simultaneous quantification of emulsion instabilities and lipid digestion kinetics, Anal. Chem. (2017), https://doi.org/10.1021/acs.analchem.7b01853.
[24] M. Golding, T.J. Wooster, The influence of emulsion structure and stability on lipid digestion, Curr. Opin. Colloid Interface Sci. 15 (2010) 90–101, https://doi.org/10.1016/j.cocis.2009.11.006.
[25] B. Greenwood-Van Meerveld, A.C. Johnson, D. Grundy, Gastrointestinal physiology and function, Handb. Exp. Pharmacol. (2017), https://doi.org/10.1007/164_2016_118.
[26] J. Campbell, J. Berry, Y. Liang, Anatomy and Physiology of the Small Intestine, Eighth Edi, Elsevier Inc., 2019. https://doi.org/10.1016/B978-0-323-40232-3.00071-6 (Chapter 71).
[27] M. Wickham, M. Garrood, J. Leney, P.D. Wilson, A. Fillery-Travis, Modification of a phospholipid stabilized emulsion interface by bile salt: effect on pancreatic lipase activity, J. Lipid Res. 39 (1998) 623–632. http://www.ncbi.nlm.nih.gov/pubmed/9548594.
[28] A.F. Hofmann, Bile acids: the good, the bad, and the ugly, Physiology 14 (1999) 24–29, https://doi.org/10.1152/physiologyonline.1999.14.1.24.
[29] A. Sarkar, A. Ye, H. Singh, On the role of bile salts in the digestion of emulsified lipids, Food Hydrocoll. (2016), https://doi.org/10.1016/j.foodhyd.2016.03.018.
[30] R. Parker, N.M. Rigby, M.J. Ridout, A.P. Gunning, P.J. Wilde, The adsorption-desorption behaviour and structure function relationships of bile salts, Soft Matter. (2014), https://doi.org/10.1039/c4sm01093k.
[31] S. Salentinig, N.R. Yepuri, A. Hawley, B.J. Boyd, E. Gilbert, T.A. Darwish, Selective deuteration for molecular insights into the digestion of medium chain triglycerides, Chem. Phys. Lipids 190 (2015) 43–50, https://doi.org/10.1016/j.chemphyslip.2015.06.007.
[32] G. Favé, T.C. Coste, M. Armand, Physicochemical properties of lipids: new strategies to manage fatty acid bioavailability, Cell. Mol. Biol. (Noisy-Le-Grand). 50 (2004) 815–831, https://doi.org/10.1170/T575.
[33] E. Bauer, S. Jakob, R. Mosenthin, Principles of physiology of lipid digestion, Asian-Australasian J. Anim. Sci. (2005), https://doi.org/10.5713/ajas.2005.282.
[34] M. Armand, P. Borel, P. Ythier, G. Dutot, C. Melin, M. Senft, H. Lafont, D. Lairon, Effects of droplet size, triacylglycerol composition, and calcium on the hydrolysis of complex emulsions by pancreatic lipase: an in vitro study, J. Nutr. Biochem. (1992), https://doi.org/10.1016/0955-2863(92)90024-D.
[35] A. Dahan, A. Hoffman, Use of a dynamic in vitro lipolysis model to rationalize oral formulation development for poor water soluble drugs: correlation with in vivo data and the relationship to intra-enterocyte processes in rats, Pharm. Res. (2006), https://doi.org/10.1007/s11095-006-9054-x.
[36] J. Calvo-Lerma, V. Fornés-Ferrer, A. Heredia, A. Andrés, In vitro digestion models to assess lipolysis: the impact of the simulated conditions of gastric and intestinal pH, bile salts and digestive fluids, Food Res. Int. 125 (2019), https://doi.org/10.1016/j.foodres.2019.108511 108511.
[37] M. Hu, Y. Li, E.A. Decker, D.J. McClements, Role of calcium and calcium-binding agents on the lipase digestibility of emulsified lipids using an in vitro digestion model, Food Hydrocoll. (2010), https://doi.org/10.1016/j.foodhyd.2010.03.010.
[38] C. Hilgendorf, H. Spahn-Langguth, C.G. Regårdh, E. Lipka, G.L. Amidon, P. Langguth, Caco-2 versus Caco-2/HT29-MTX Co-cultured Cell Lines: Permeabilities Via Diffusion, Inside- and Outside-Directed Carrier-Mediated Transport, J. Pharm. Sci. 89 (2000) 63–75, https://doi.org/10.1002/(SICI)1520-6017(200001)89:1<63::AID-JPS7>3.0.CO;2-6.
[39] G.J. Mahler, M.L. Shuler, R.P. Glahn, Characterization of Caco-2 and HT29-MTX cocultures in an in vitro digestion/cell culture model used to predict iron bioavailability☆, J. Nutr. Biochem. 20 (2009) 494–502, https://doi.org/10.1016/j.jnutbio.2008.05.006.
[40] P. Artursson, K. Palm, K. Luthman, Caco-2 monolayers in experimental and theoretical predictions of drug transport, Adv. Drug Deliv. Rev. (2012), https://doi.org/10.1016/j.addr.2012.09.005.
[41] L.M. Ensign, R. Cone, J. Hanes, Oral drug delivery with polymeric nanoparticles: The gastrointestinal mucus barriers, Adv. Drug Deliv. Rev. 64 (2012) 557–570, https://doi.org/10.1016/j.addr.2011.12.009.
[42] S. May, C. Hirsch, A. Rippl, N. Bohmer, J.-P. Kaiser, L. Diener, A. Wichser, A. Bürkle, P. Wick, Transient DNA damage following exposure to gold nanoparticles, Nanoscale. 10 (2018) 15723–15735, https://doi.org/10.1039/C8NR03612H.
[43] Alcian Blue Staining Protocol, (n.d.). http://www.ihcworld.com/_protocols/special_stains/alcian_blue.htm (accessed November 4, 2019).
[44] C. Jumarie, C. Malo, Caco-2 cells cultured in serum-free medium as a model for the study of enterocytic differentiation in vitro, J. Cell. Physiol. 149 (1991) 24–33, https://doi.org/10.1002/jcp.1041490105.
[45] T. Lea, Caco-2 Cell Line, in: Impact Food Bioact. Heal., Springer International Publishing, Cham, 2015: pp. 103-111. https://doi.org/10.1007/978-3-319-16104-4_10.
[46] L. Vila, A. García-Rodríguez, C. Cortés, A. Velázquez, N. Xamena, A. Sampayo-Reyes, R. Marcos, A. Hernández, Effects of cerium oxide nanoparticles on differentiated/undifferentiated human intestinal Caco-2 cells, Chem. Biol. Interact. 283 (2018) 38–46, https://doi.org/10.1016/j.cbi.2018.01.018.
[47] M. Kucki, L. Diener, N. Bohmer, C. Hirsch, H.F. Krug, V. Palermo, P. Wick, Uptake of label-free graphene oxide by Caco-2 cells is dependent on the cell differentiation status, J. Nanobiotechnol. 15 (2017) 1–18, https://doi.org/10.1186/s12951-017-0280-7.
[48] A.H. Henkin, A.S. Cohen, E.A. Dubikovskaya, H.M. Park, G.F. Nikitin, M.G. Auzias, M. Kazantzis, C.R. Bertozzi, A. Stahl, Real-time noninvasive imaging of fatty acid uptake in vivo, ACS Chem. Biol. 7 (2012) 1884–1891, https://doi.org/10.1021/cb300194b.
[49] N. Navabi, M.A. McGuckin, S.K. Lindén, Gastrointestinal cell lines form polarized epithelia with an adherent mucus layer when cultured in semi-wet interfaces with mechanical stimulation, PLoS One 8 (2013), https://doi.org/10.1371/journal.pone.0068761 e68761.
[50] C. Schimpel, B. Teubl, M. Absenger, C. Meindl, E. Fröhlich, G. Leitinger, A. Zimmer, E. Roblegg, Development of an advanced intestinal in vitro triple culture permeability model to study transport of nanoparticles, Mol. Pharm. 11 (2014) 808–818, https://doi.org/10.1021/mp400507g.
[51] G.J. Mahler, M.B. Esch, E. Tako, T.L. Southard, S.D. Archer, R.P. Glahn, M.L. Shuler, Oral exposure to polystyrene nanoparticles affects iron absorption, Nat. Nanotechnol. 7 (2012) 264–271, https://doi.org/10.1038/nnano.2012.3.
[52] Z. Guo, N.J. Martucci, F. Moreno-Olivas, E. Tako, G.J. Mahler, Titanium dioxide nanoparticle ingestion alters nutrient absorption in an in vitro model of the small intestine, NanoImpact. 5 (2017) 70–82, https://doi.org/10.1016/j.impact.2017.01.002.
[53] F. Antunes, F. Andrade, F. Araújo, D. Ferreira, B. Sarmento, Establishment of a triple co-culture in vitro cell models to study intestinal absorption of peptide drugs, Eur. J. Pharm. Biopharm. 83 (2013) 427–435, https://doi.org/10.1016/j.ejpb.2012.10.003.
[54] E. Brun, F. Barreau, G. Veronesi, B. Fayard, S. Sorieul, C. Chanéac, C. Carapito, T. Rabilloud, A. Mabondzo, N. Herlin-Boime, M. Carrière, Titanium dioxide nanoparticle impact and translocation through ex vivo, in vivo and in vitro gut epithelia, Part. Fibre Toxicol. 11 (2014) 13, https://doi.org/10.1186/1743-8977-11-13.
[55] C. Atuma, V. Strugala, A. Allen, L. Holm, The adherent gastrointestinal mucus gel layer: thickness and physical state in vivo, Am. J. Physiol. Liver Physiol. 280 (2001) G922–G929, https://doi.org/10.1152/ajpgi.2001.280.5.G922.
[56] H.H. Sigurdsson, J. Kirch, C.-M. Lehr, Mucus as a barrier to lipophilic drugs, Int. J. Pharm. 453 (2013) 56–64, https://doi.org/10.1016/J.IJPHARM.2013.05.040.
[57] J. Keemink, C.A.S. Bergström, Caco-2 cell conditions enabling studies of drug absorption from digestible lipid-based formulations, Pharm. Res. 35 (2018) 74, https://doi.org/10.1007/s11095-017-2327-8.
[58] C. Ortiz, M.L. Ferreira, O. Barbosa, J.C.S. dos Santos, R.C. Rodrigues, Á. Berenguer-Murcia, L.E. Briand, R. Fernandez-Lafuente, Novozym 435: the "perfect" lipase immobilized biocatalyst?, Catal. Sci. Technol. 9 (2019) 2380–2420, https://doi.org/10.1039/C9CY00415G.
[59] G.M. DeLoid, Y. Wang, K. Kapronezai, L.R. Lorente, R. Zhang, G. Pyrgiotakis, N.V. Konduru, M. Ericsson, J.C. White, R. De La Torre-Roche, H. Xiao, D.J. McClements, P. Demokritou, An integrated methodology for assessing the impact of food matrix and gastrointestinal effects on the biokinetics and cellular toxicity of ingested engineered nanomaterials, Part. Fibre Toxicol. 14 (2017) 1–17, https://doi.org/10.1186/s12989-017-0221-5.
[60] A. des Rieux, V. Fievez, M. Garinot, Y.J. Schneider, V. Préat, Nanoparticles as potential oral delivery systems of proteins and vaccines: a mechanistic approach, J. Control. Release (2006). https://doi.org/10.1016/j.jconrel.2006.08.013.
[61] W.J. Lossow, F.T. Lindgren, J.C. Murchio, G.R. Stevens, L.C. Jensen, Particle size and protein content of six fractions of the Sf 20 plasma lipoproteins isolated by density gradient centrifugation, J. Lipid Res. 10 (1969) 68–76.
[62] D.P. Cistola, J.A. Hamilton, D. Jackson, D.M. Small, Ionization and phase behavior of fatty acids in water: application of the Gibbs phase rule, Biochemistry. 27 (1988) 1881–1888, https://doi.org/10.1021/bi00406a013.
[63] R. Negrini, R. Mezzenga, pH-responsive lyotropic liquid crystals for controlled drug delivery, Langmuir. 27 (2011) 5296–5303, https://doi.org/10.1021/la200591u.
[64] A. Salonen, C. Moitzi, S. Salentinig, O. Glatter, Material transfer in cubosome−emulsion mixtures: effect of alkane chain length, Langmuir 26 (2010) 10670–10676, https://doi.org/10.1021/la100955z.
[65] T.F. Whayne, J.M. Felts, Activation of lipoprotein lipase. Evaluation of calcium, magnesium, and ammonium as cofactors, Circ. Res. (1971), https://doi.org/10.1161/01.RES.28.6.649.
[66] H. Kimura, Y. Futami, S.I. Tarui, T. Shinomiya, Activation of human pancreatic lipase activity by calcium and bile salts, J. Biochem. (1982), https://doi.org/10.1093/oxfordjournals.jbchem.a133920.
[67] M. Mukherjee, Human digestive and metabolic lipases - a brief review, J. Mol. Catal. B Enzym. (2003), https://doi.org/10.1016/S1381-1177(03)00052-3.
[68] D.J. McClements, Encapsulation, protection, and delivery of bioactive proteins and peptides using nanoparticle and microparticle systems: a review, Adv. Colloid Interface Sci. 253 (2018) 1–22, https://doi.org/10.1016/j.cis.2018.02.002.
[69] M. Koziolek, F. Carrière, C.J.H. Porter, Lipids in the stomach - implications for the evaluation of food effects on oral drug absorption, Pharm. Res. (2018), https://doi.org/10.1007/s11095-017-2289-x.
[70] C.W. Pouton, Formulation of poorly water-soluble drugs for oral administration: Physicochemical and physiological issues and the lipid formulation classification system, Eur. J. Pharm. Sci. (2006), https://doi.org/10.1016/j.ejps.2006.04.016.